Ecologica Montenegrina
ISSN 2336-9744 (online) | ISSN 2337-0173 (print)

Ecologica Montenegrina 103: 136-154 (2026)
This journal is available online at: www.biotaxa.org/em
https://dx.doi.org/10.37828/em.2026.103.9

Article

Otolith microchemistry of three deep-sea rockfishes (Scorpaeniformes, Sebastidae) from the Emperor Seamount Chain

NIKOLAI B. KOROSTELEV[1]*, VLADIMIR V. BELYAKOV[1], VASILISA B. BARANOVSKAYA[2], NATALIA A. KOROTKOVA[2], LYUDMILA S. ZINEVICH[1], IGOR V. MALTSEV[3], GRIGORII N. MARKEVICH[1] & ALEXEI M. ORLOV[4,1,5]

[1]*A.N. Severtsov Institute of Ecology and Evolution of the Russian Academy of Sciences, Moscow, Russia.*
E-mail: vovafromperovo@yandex.ru; https://orcid.org/0000-0003-3786-3558
E-mail: lzinevich@gmail.com; https://orcid.org/0000-0001-5214-5744
E-mail: g-markevich@yandex.ru; https://orcid.org/0000-0002-6893-4286
[2]*Kurnakov Institute of General and Inorganic Chemistry of the Russian Academy of Sciences, Moscow, Russia.*
E-mail: baranovkova@list.ru; https://orcid.org/0000-0002-0076-9990
E-mail: natalya.korotkova.95@mail.ru; https://orcid.org/0000-0003-1269-6570
[3] *Pacific branch of the Russian Federal Research Institute of Fisheries and Oceanography, Vladivostok, Russia.*
E-mail: maltsev.8766@mail.ru; https://orcid.org/0000-0003-0540-2837
[4]*Shirshov Institute of Oceanology, Russian Academy of Sciences, Moscow, Russia.*
E-mail: orlov.am@ocean.ru; https://orcid.org/0000-0002-0877-2553
[5]*Tomsk State University, Tomsk, Russia.*
**Corresponding author. E-mail: korostelevnb@gmail.com; https://orcid.org/0000-0002-9452-3704*

Received 5 October 2026 | Accepted by *V. Pešić*: 8 November 2026 | Published online 19 November 2026.

Abstract
This study presents a comparative analysis of otolith elemental composition in three deep-sea rockfish species from the Emperor Seamount Chain: *Sebastes iracundus* (performs regular vertical migrations), *Helicolenus avius* and *Adelosebastes latens* (non-migratory species). Concentrations of 25 elements were determined by mass and optical emission spectrometry (ICP-MS/OES). Kruskal-Wallis tests revealed significant differences among the three species for 20 of the 24 analyzed elements ($p<0.05$), and pairwise comparisons (Dunn's test) showed that the majority of these differences separated *S. iracundus* from both sedentary species. Hierarchical clustering (Ward.D2) also demonstrated this strong *S. iracundus* separation, whereas *H. avius* and *A. latens* were largely similar. PERMANOVA ($F_{2,11}=46.39$, $R^2=0.894$, $p=0.001$) confirmed a strong influence of species identity on otolith element composition. SIMPER analysis identified Zn, Y, Rb, Sc, and Ce as the principal contributors to the dissimilarity between *S. iracundus* and the sedentary species. In contrast, the separation between *H. avius* and *A. latens* was driven primarily by Ti. These results suggest that the distinct otolith signature of *S. iracundus* reflects a combination of extrinsic factors (contact with contrasting water masses during vertical migrations) and intrinsic factors (physiological regulation and diet), whereas the finer-scale separation between the two sedentary species is more likely environmental.

Key words otolith composition, ICP-MS, ICP-OES, vertical migration, *Sebastes iracundus, Helicolenus avius, Adelosebastes latens*.

© 2026 The Author(s). This is an open access article distributed under the terms of the Creative Commons Attribution License (CC BY), which permits unrestricted use, distribution, and reproduction in any medium, provided the original author and source are credited.

Introduction

Otoliths, or earstones, are calcium carbonate structures found in the inner ear and involved in hearing and balance. They are traditionally utilized by marine biologists in numerous ways, including age determination (Campana, 2001; Korostelev et al., 2020), morphological shape analysis (Afanasyev et al., 2017; Tuset et al., 2016), and chemical analysis (Campana, 1999; Reis-Santos et al., 2023). As otoliths grow throughout fish ontogeny, accumulating chemical elements from the environment while remaining otherwise metabolically inert, their chemical composition bears information about the conditions the fish experienced (Campana, 1999). Therefore, otolith composition data can be used to distinguish between fish populations from different areas (stock delineation) (Campana et al., 2000; Thorrold et al., 2001), reconstruct the chronology of anadromous fish movements between fresh and salt waters (Gillanders, 2005; Secor and Rooker, 2000), determine temperature conditions of habitat (Høie et al., 2004), and validate age determinations (Smith et al., 1991; Kastelle et al., 2020;).

Although otolith chemical analysis has proven to be a useful tool in numerous studies of shallow-water species, its application in studies of deep-sea fishes remains relatively scarce (Longmore et al., 2011; Korostelev and Orlov, 2020; Santificetur et al., 2026). At the same time, the method appears to be one of the few that provide reliable information on the group's biology and lifestyle (Farias et al., 2022; Wu et al., 2024; Widdrington et al., 2025; Santificetur et al., 2026).

This study is dedicated to the otolith composition of several deep-sea rockfishes of the family Sebastidae. The family represents one of the most diverse groups of teleost fishes in the North Pacific (Snytko, 2001; Love et al., 2002; Barsukov, 2003) and includes 7 genera and more than 130 species (Froese and Pauly, 2026). A key factor in speciation within this group has been differentiation by depth of habitat, which was accompanied by the development of specialized morphological, physiological, and sensory adaptations (Love et al., 2002; Ingram, 2011; Tuset et al., 2016).

The chemical composition of Sebastidae otoliths has already been addressed in several studies. Thus, for *Sebastes marinus*, *S. mentella, S. melanops*, and *Helicolenus dactylopterus*, weak geographic differences in otolith composition have been demonstrated (Stransky, 2004; Miller et al., 2005; Swan et al., 2006). For redfishes of the North Atlantic, ontogenetic changes in Sr and Ba levels were revealed (Stransky et al., 2005). Furthermore, a paper on a deep-water representative of the family, *H. dactylopterus*, has shown the possibility of discriminating regional groups based on element sets (Higgins et al., 2013). The present study supplements information on Sebastidae otolith composition, providing the first such data for three deep-sea species.

Materials and Methods

Objects of study

For this study, three closely related deep-sea rockfish species with different life styles were selected (Fig. 1). *Sebastes iracundus* (Jordan et Starks, 1904) is a viviparous species characterized by a wide bathymetric range (200–1,400 m) (Orlov and Tokranov, 2019) and the ability to perform vertical migrations, as evidenced by data on diel catch dynamics (Orlov and Tokranov, 2006, 2007; Kurbanov, 2025). Like other representatives of the genus *Sebastes*, this species possesses a closed swim bladder. *Helicolenus avius* Abe et Eschmeyer, 1972 is also a viviparous species, inhabiting significantly shallower depths in the Emperor Seamounts area (290–600 m) (NPFC, 2024). Information on its vertical movements is lacking; however, given the loss of the swim bladder in the ancestors of the genus *Helicolenus* during early stages of their evolution (Barsukov, 1981), a predominantly benthic lifestyle can be assumed. *Adelosebastes latens* Eschmeyer, Abe et Nakano, 1979 is a member of a monotypic genus, leading a sedentary benthic lifestyle at great depths (350–1,200 m). This species lacks a swim bladder (Kurbanov and Mikhalyutin, 2022) and is oviparous with internal fertilization, which fundamentally distinguishes it from the other two species (Orr and Baker, 1996; Kurbanov and Mikhalyutin, 2022). The studied species are of commercial importance, being caught in the Emperor Seamounts area as bycatch in the longline fishery for the skilfish *Erilepis zonifer* (Korostelev et al., 2025; Orlov and Tuponogov, 2026).

Sample collection and species identification

Sagittal otoliths of rockfishes (Sebastidae) were sampled from catches of commercial longliner "Palmer" (Yuzhny Krest LLC, Petropavlovsk-Kamchatsky, Russia) in the Emperor Seamounts area (northwestern Pacific). Otoliths from four individuals of *Sebastes iracundus* and five individuals of *Adelosebastes latens*, caught at a depth of 880 m in the waters of Jingu Seamount (38°50′00″N 171°15′00″E), and five individuals of *Helicolenus avius*, caught at a depth of 600 m on Koko Seamount (35°15′00″N 171°34′48″E) were analyzed.

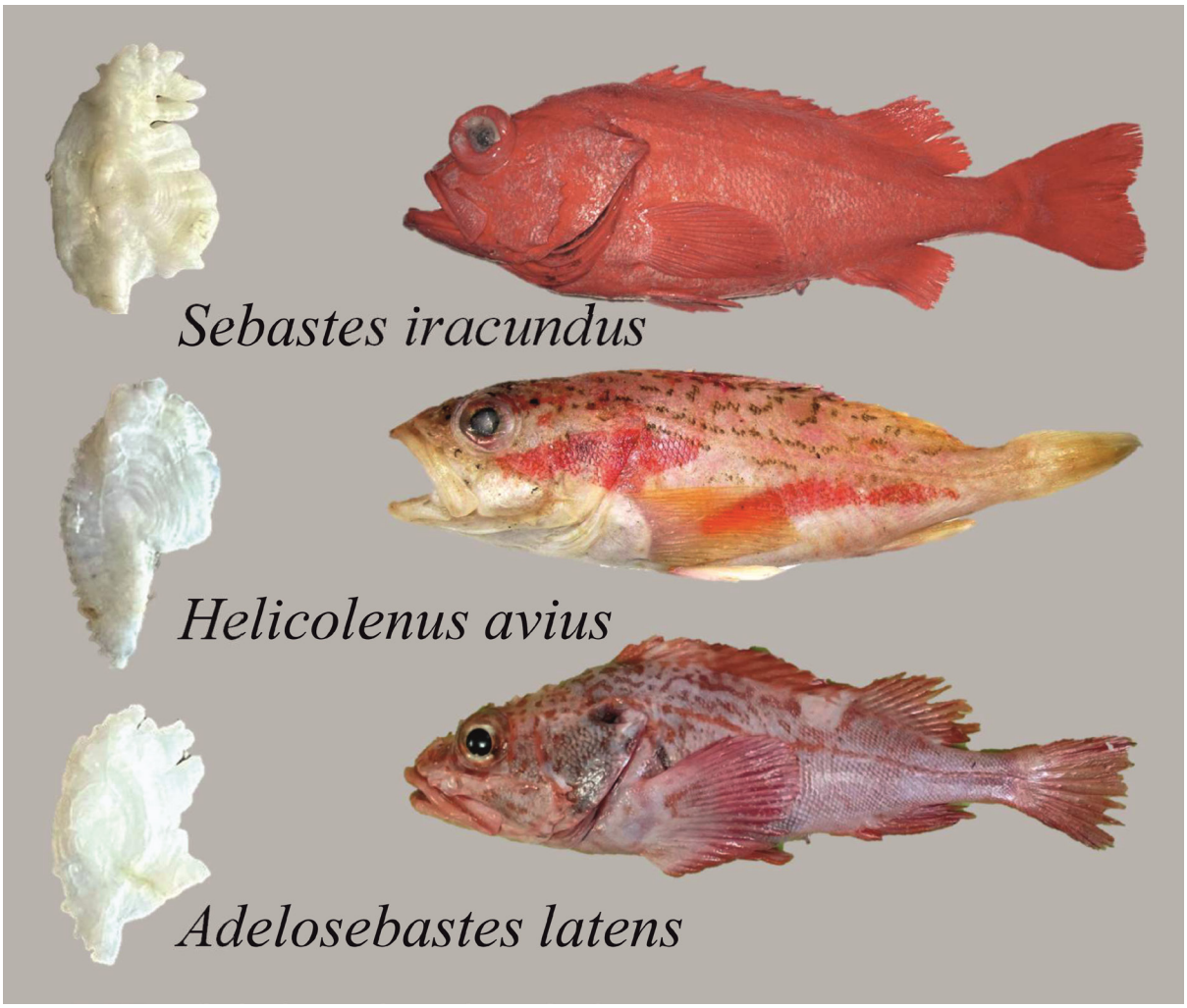


Figure 1. Appearance of three rockfishes *Sebstes iracundus*, *Helicolenus avius* and *Adelosebastes latens* (right) and their otoliths (left). Fish images by A.M. Orlov.

Determination of the elemental composition of otoliths

The elemental composition of the otoliths was analyzed using inductively coupled plasma optical emission spectroscopy (ICP-OES) and mass spectrometry (ICP-MS). ICP-OES was performed using the iCAP PRO XP spectrometer (Thermo Scientific, USA) (Table 1).

The ICP-MS analysis was performed using the Supec 7000 mass spectrometer (Focused Photonics, China) (Table 2).

The samples were prepared using an autoclave system equipped with microwave treatment capabilities. Otolith processing was conducted using the MARS 6 laboratory system (CEM Corp., USA). For the experiment, Easy-Prep iWave vessels were utilized. These containers facilitated the heating of aqueous solutions of concentrated acids at high temperatures. A 50% HNO_3 solution, prepared from high-purity HNO_3 (HNO_3 – 70%) and deionized water, was used to process the samples in the microwave oven. The DST-1000 (Savillex, USA) was used to further purify HNO_3 before preparing all solutions. Deionized water with a resistivity of 18.2 MΩ·cm at 25°C was used to dilute all solutions.

The solution volume was 10 ml, the sample mass was 100 – 200 mg, and the processing parameters included a ramp-up time of 10 minutes, a hold time of 30 minutes at 200°C, an output power of 1500 W, and a cooling time of 15 minutes. Corresponding technological blanks without a sample were prepared using the identical process, ensuring they were treated identically to the samples. The blank results were averaged and taken into account during the processing of the otolith analysis results. Aqueous calibration solutions were prepared using multi-element and single-element standards (High-Purity Standards, USA). The solutions were serially diluted to various volumes using a 2% HNO_3 mixture. For ICP-OES, calibration solutions were formulated within the concentration ranges of 0.1–50 mg/L for Na, P, K, and Sr, and 0.1–300 mg/L for Ca. In the case of ICP-MS, calibration solutions were prepared across the ranges of 0.1–50 μg/L for Li, B, Mg, Al, Ti, Cr, Mn, Fe, Co, Ni, Cu, Zn, Ga, Ge, Rb, Y, Ba and 0.01–10 μg/L for Sc, La, Ce. Prior to measurement, all solutions were further diluted tenfold for ICP-OES and twentyfold for ICP-MS. The number of analytical replicates was 3. The trueness of the obtained results was confirmed using the "added-found" method.

Table 1. Operating parameters of the optical-emission spectrometer.

Forward power, W	1300
Coolant gas flow, L·min^{-1}	15
Auxiliary gas flow, L·min^{-1}	0.35
Nebuliser gas flow, L·min^{-1}	0.6
Sample flow rate, rpm	60
Pump tube, mm	0.64
Radial viewing height, mm	10
Injector diameter, mm	2
Wavelengths of determined elements, nm	Na 589.592; Si 251.611; P 213.618, 185.942; K 766.490; Ca 396.847, 422.673; Sr 407.771

Table 2. Operating parameters of the mass-spectrometer.

Forward power, W	1550
Coolant gas flow, L·min^{-1}	14.0
Auxiliary gas flow, L·min^{-1}	1.0
Nebulizer gas flow, L·min^{-1}	1.05
Sample flow rate, rpm	30
Helium flow rate (KED mode), mL·min^{-1}	2.0
Level of oxide ions, %	<2.0
Level of doubly charged ions, %	<2.0
Measurement mode	Peak hopping
Isotopes of determined elements, m/z	^{7}Li, ^{9}B, ^{24,25}Mg, ^{27}Al, ^{45}Sc, ^{49}Ti, ^{55}Mn, ^{56,57}Fe (KED mode), ^{59}Co, ^{60,61}Ni, ^{63,65}Cu, ^{66,67}Zn, ^{69}Ga, ^{72}Ge, ^{85}Rb, ^{89}Y, ^{137}Ba, ^{139}La, ^{140}Ce
Internal standard	^{103}Rh, ^{115}In

Statistical analysis

Statistical analyses were performed in the R environment (version 4.5.1; R Core Team 2025). For all elements, bulk element/Ca mass ratios were calculated and subsequently log-transformed to normalize the distribution (Aitchison, 1986). Values below the detection limit were treated using multivariate imputation implemented in the zCompositions package (Palarea-Albaladejo and Martín-Fernández, 2015), which allowed the preservation of the correlation structure among elements in accordance with compositional data analysis principles. To identify differences in individual element concentrations among species, the non-parametric Kruskal–Wallis test was used (Kruskal and Wallis, 1952), followed by pairwise comparisons using Dunn's test (Dunn, 1964) with Holm's correction (Holm, 1979) for multiple comparisons.

To assess the multivariate structure of the data, Euclidean distances were calculated between individuals based on the log10-transformed element/Ca ratios. Agglomerative hierarchical clustering was performed using the Ward.D2 linkage method (stats; Ward, 1963). Statistically significant

differences in multivariate elemental composition among species were tested through permutational multivariate analysis of variance (PERMANOVA) with 999 permutations (vegan; Anderson, 2001; McArdle and Anderson, 2001). The coefficient of determination R^2 was used as a measure of effect size, indicating the proportion of variance explained by species identity. Similarity percentage analysis (SIMPER; Clarke, 1993) was conducted to identify which elements contributed most to the dissimilarity between species pairs. SIMPER analysis was performed using the simper() function in the vegan package, which implements the Bray-Curtis dissimilarity index, a standard metric for this procedure. To complement the log-transformed SIMPER analysis, a second SIMPER was performed on the untransformed element/Ca ratios. This approach quantifies the absolute contribution of each element to between-group dissimilarity, in contrast to the log-transformed analysis, which identifies elements contributing to the multivariate structure after variance compression.

Results

Our analyses determined the content of 25 elements in otoliths of three rockfish species (*S. iracundus, H. avius, A. latens*) (Fig. 2b; Table S1). Ca was the main component in all samples, with mean mass concentrations ranging from 371,220 ± 4,209 ppm in *H. avius* to 377,540 ± 5,289 ppm in *A. latens*. The contents of Na, Sr, and P were significantly lower, ranging from several hundred to 3,000 ppm. Concentrations of K, Si, Fe, Ba, Mg, Al, and Zn ranged from tens to hundreds of ppm. Ti, Ni, Li, Mn, Cu, Co, B, Y, La, Ce, Ga, Ge, Rb and Sc occurred in trace amounts (< 6 ppm). Not all of the analyzed elements were detected in all three species: Rb, Sc, Ge, and Ga were measurable only in *S. iracundus*, whereas their concentrations in *H. avius* and *A. latens* were below the detection limit. Conversely, Zn, Y, and La could not be measured in *S. iracundus*, and Ce was detected in only one *S. iracundus* otolith at a particularly low concentration. These elements were nevertheless retained for further statistical analysis, with the missing values imputed using the zCompositions package and the known detection limit.

A series of Kruskal-Wallis tests, performed on log-transformed element-to-calcium mass ratios, revealed statistically significant differences among the three species for 20 out of 24 analyzed elements (Table S2). No significant differences were detected for Fe, B, Cu, and Ge. Pairwise comparisons (Dunns test with Holm's correction) showed that the greatest number of significant differences occurred between *S. iracundus* and the other two species (14 and 11), whereas *H. avius* and *A. latens* exhibited similarity, with the differences in all elements remaining insignificant (Table S3).

Hierarchical clustering (Ward.D2) conducted on logarithms of element/Ca ratios separated all three species into distinct branches (Fig. 3). *H. avius* and *A. latens* were more similar to each other, merging at a substantially lower Euclidean distance, while *S. iracundus* separated from this clade at the highest linkage distance. Permutational multivariate analysis of variance (PERMANOVA) confirmed statistically significant differences in elemental composition among the studied species ($F_{2,11} = 46.39$, $R^2 = 0.894$, $p = 0.001$), with species identity explaining 89.4% of the total multivariate variance. The effect size indicates a strong separation, far exceeding the within-species variance. Furthermore, SIMPER analysis identified the elements contributing most to the dissimilarity between species (Fig. 4, Table S4). The distribution of elements' dissimilarity contributions was similar when comparing *S. iracundus* with the other two species. Because the analysis was performed on log-transformed ratios, the dominant elements (Na, Sr) did not overshadow the trace elements, as they did in the untransformed dataset (Fig. S1). Consequently, Zn/Ca was the largest contributor to the dissimilarity between *S. iracundus* and both sedentary species (9.5% in both comparisons), followed by Y/Ca (8.1–8.3%), La/Ca (6.5–8.1%), Rb/Ca (7.0–7.1%), Sc/Ca (6.7%), and Ce/Ca (6.6%). Na/Ca and Sr/Ca, which dominated when untransformed ratios were analyzed, contributed only 5.2–6.1% each in the log-transformed dataset. In contrast, the dissimilarity between the two sedentary species was dominated by Ti/Ca (16.3%, $p = 0.023$), whereas all other elements showed no statistically significant contribution ($p > 0.84$). Overall, SIMPER confirmed the results of univariate comparisons: 20 and 21 elements contributed significantly ($p < 0.05$) to the dissimilarity between *S. iracundus* and *H. avius*, and between *S. iracundus* and *A. latens*, respectively. In contrast, only one element (Ti/Ca) was significant in the *H. avius* vs *A. latens* comparison.

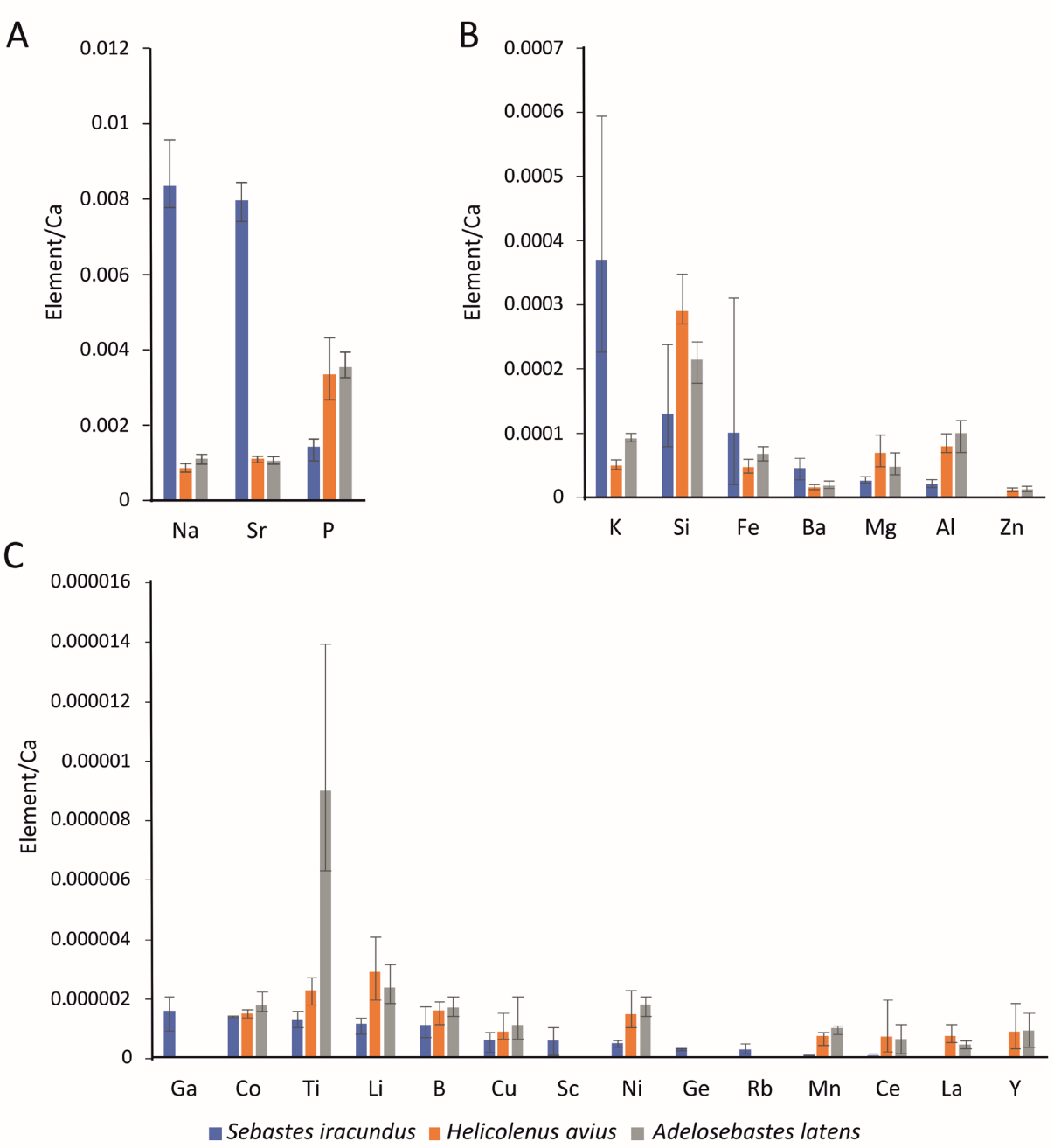


Figure 2. Elemental composition of otoliths of three rockfishes (*S. iracundus*, *H. avius* and *A. latens*) from the Emperor Seamount Chain showing mean, minimum, and maximum mass ratios of A) minor elements to Ca; B,C) trace elements to Ca.

Discussion

Both single-element pairwise comparisons (Dunn's test with Holm's correction) and multivariate analysis utilizing data on 24 detected elements show similarity between the otolith compositions of *H. avius* and *A. latens*, with *S. iracundus* distinctly differing from both. As the former two species were collected at different depths and seamounts, the observed pattern does not appear to be driven solely by their immediate habitats. Therefore, while the modest sample sizes and uneven geographical distribution of catches prevent us from drawing any firm conclusions, we still suggest that these results reflect real ecological differences between the species. Among the studied species, *S. iracundus* is characterized by the widest bathymetric range (200–1,400 m) (Orlov and Tokranov, 2019) and the ability to perform

vertical migrations, as evidenced by data on diel catch dynamics (Orlov and Tokranov, 2006, 2007; Kurbanov 2025). Such movements through the water column imply contact with water masses differing in temperature and hydrochemical characteristics. At the same time, the physiological processes taking place during these migrations can also affect accumulation of some elements. Therefore, we believe that both extrinsic and intrinsic factors contribute to the distinctive otolith composition of *S. iracundus*.

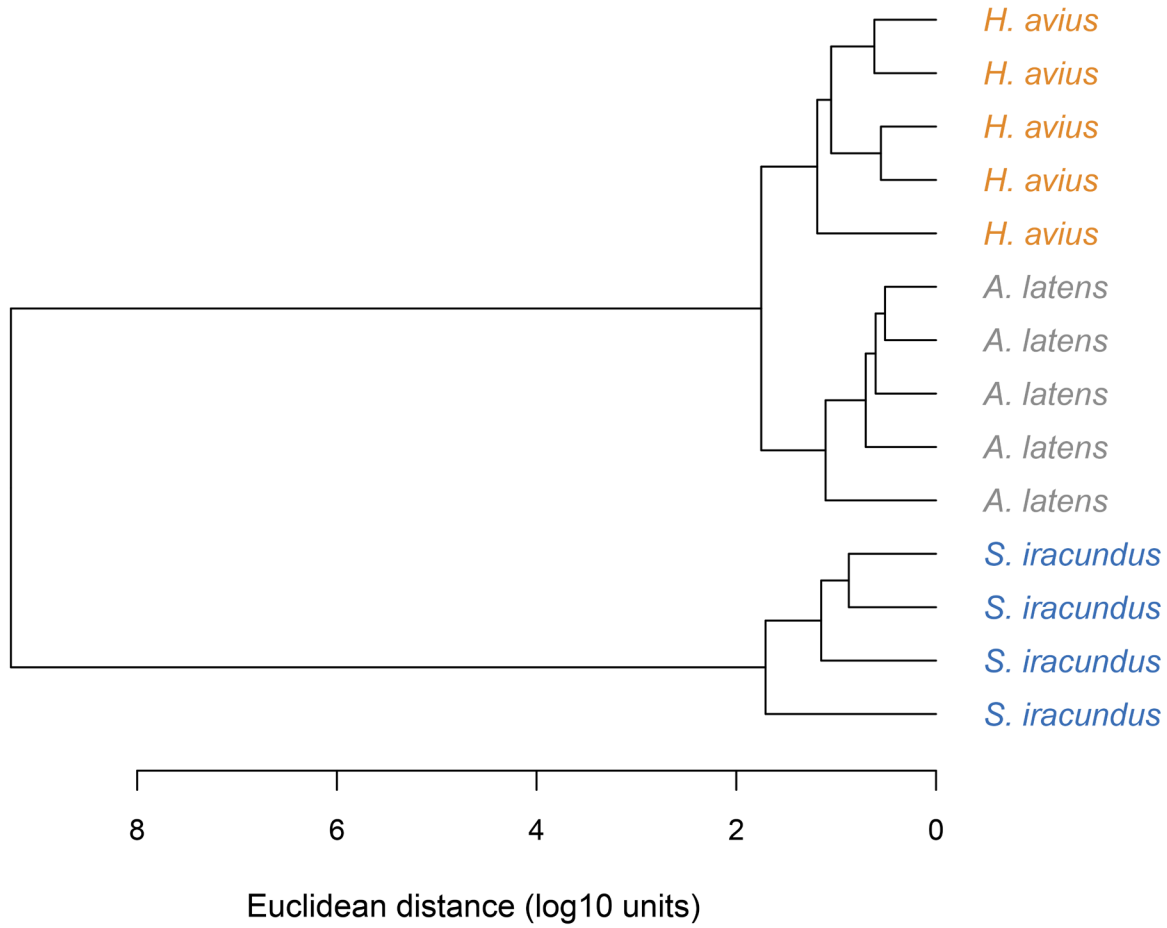


Figure 3. Hierarchical clustering of otolith elemental composition in three rockfish species from the Emperor Seamount Chain. The dendrogram was constructed using Ward.D2 linkage based on Euclidean distances among log10-transformed element/Ca ratios. Each terminal branch represents one individual. Font colors denote species.

The distinctiveness of the *S. iracundus* otolith composition is supported by the fact that its differences from both *H. avius* and *A. latens* are reflected by the vast majority of the analyzed elements. Such a broad elemental signature indicates that the separation of the species is not driven by a few outlier elements but represents a complex, multi-element shift in otolith chemistry. The most pronounced differences in absolute element concentrations between *S. iracundus* and the other two species were found in Sr, Na and K levels and confirmed by a SIMPER analysis on untransformed data. While otolith Sr level is considered to "honestly" reflect its concentration in the environment (Campana, 1999), its uptake also depends on water temperature and salinity (Tzeng et al., 1997; Bath et al., 2000; Martin et al., 2004). In the Emperor Seamounts area, a pronounced salinity minimum forms at depths of 500–700 m, with higher salinity levels typical of the upper water layers (Hicks et al., 2025). Regular vertical migrations to these layers may be the driver of the relatively high Sr level in *S. iracundus* otoliths, although without direct salinity measurements this remains speculative. Ba, another environmental tracer, also tends to be higher in *S. iracundus* possibly reflecting its movement pattern, as the element's abundance has been shown to generally decrease with depth (Widdrington et al., 2025; Santificetur et al., 2026). On the other hand, otolith Na and K concentrations are weakly connected with their levels in the ambient water (Campana, 1999; Reis-Santos et al., 2023), since their ions are subject to strict

physiological control. The observed interspecific differences in otolith concentrations of these elements may be evidence of the physiological changes taking place in the *S. iracundus* organism during its migrations, although their interpretation is limited due to Na^+ and K^+ playing important roles in many different processes (Kalish, 1989).

By contrast, SIMPER analysis of log-transformed ratios mitigated the overwhelming influence of absolute concentration differences (which span several orders of magnitude between major and trace elements), allowing an unbiased comparison of the elements' contributions to multivariate dissimilarity. According to the results of this analysis, the separating role of Na, K, and Sr was relatively moderate, whereas elements such as Zn, Y, La, Rb, Sc, and Ce contributed more strongly to the dissimilarity of *S. iracundus* from the sedentary species. Notably, these elements' concentrations were found to be below the detection limit in either *S. iracundus* (Zn, Y, La, Ce) or the other species (Rb, Sc, along with Ga and Ge). Therefore, the high contributions of these elements to the SIMPER dissimilarity reflect a qualitative difference in elemental occurrence (presence vs. absence) rather than a quantitative difference in concentration.

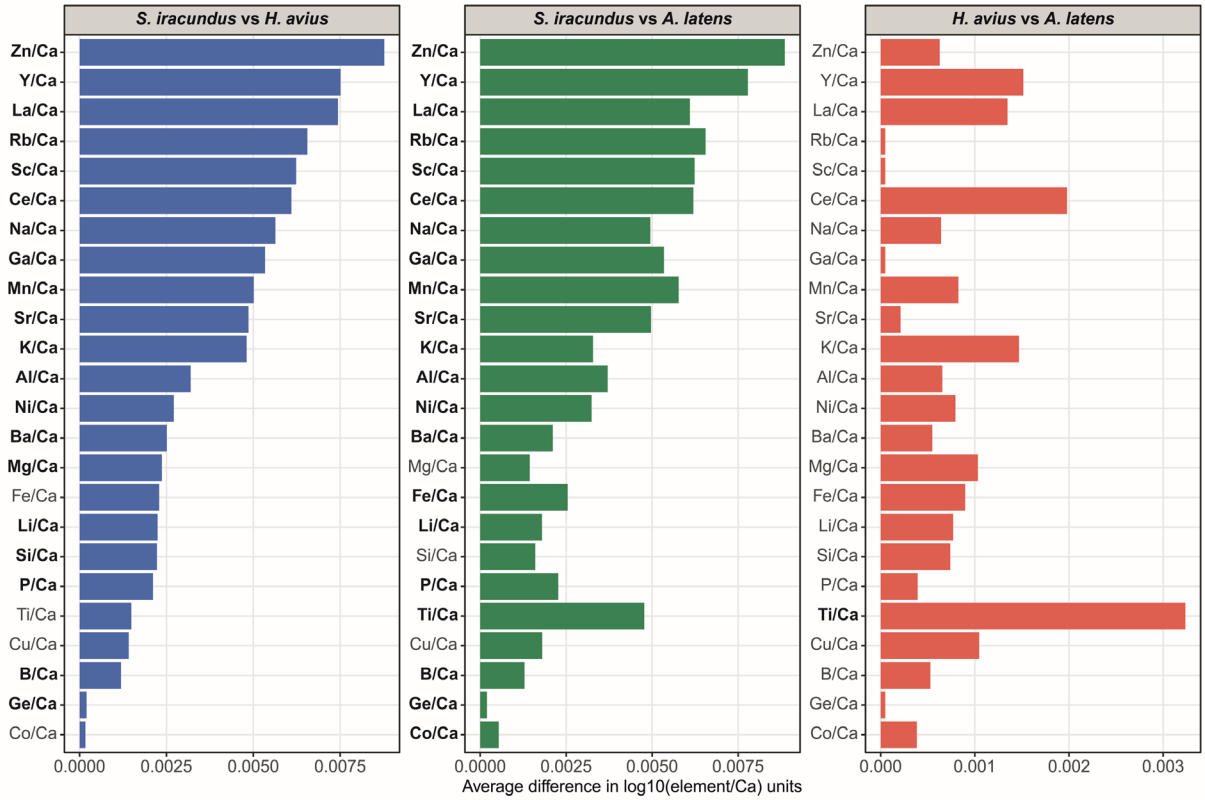


Figure 4. SIMPER analysis of otolith elemental composition among three rockfish species. Bars show the average contribution of each log10-transformed element/Ca ratio to the total between-species dissimilarity (Bray-Curtis index). Panels correspond to pairwise species comparisons; colors indicate the specific species pair; note that the scale is not consistent across panels. Elements are ordered according to their contribution in the *S. iracundus* vs *H. avius* comparison and remain in the same order across panels. Elements with statistically significant ($p<0.05$) contributions are written in bold.

La, Ce, and Y belong to the rare-earth elements (REEs), which typically occur in fish otoliths at extremely low levels (Elderfield and Pagett, 1986) and are therefore rarely analyzed. However, experimental feeding of captive fish with a REE-rich diet led to measurable accumulation of these elements in their hard tissues, although the low digestibility of the supplemented REEs suggested that incorporation may occur via direct absorption from the water (Pérez de Nanclares et al., 2014). REEs form stable carbonate and bicarbonate complexes in seawater (Elderfield and Pagett, 1986; Dub and Mizens, 2023). Zhang et al. (1994) demonstrated that Y in the North Pacific exhibits a nutrient-like depth profile, with concentrations increasing from the surface to the lower layers, closely resembling the profile of the heavier REEs. In our study, the presence of Y, La and Ce only in the sedentary species

(*H. avius* and *A. latens*), inhabiting depths of 600–900 m, is consistent with this depth-related enrichment. The migratory *S. iracundus*, which regularly traverses the water column and may feed in surface waters where Y concentrations are lower, may not accumulate sufficient Y for detection in the otolith. Conversely, Sc, although formally classified as a REE, differs from lanthanides in its ionic radius and complexation behavior (Dub and Mizens, 2023). The contrasting presence of Sc only in *S. iracundus* confirms that Sc, unlike Y, does not follow the carbonate-complexation pathway typical of heavy REEs (Zhang et al., 1994) and may be incorporated via a different mechanism.

Rb is rarely used as an otolith tracer, and to our knowledge, its incorporation has been explicitly documented in only a few studies, such as the work of Friedrich and Halden (2008), who showed that Rb concentrations in otoliths can reflect local geological signatures. Given this limited evidence base, the presence of Rb only in the migratory *S. iracundus* in our study is difficult to interpret.

Zn, in contrast, is well studied and is a classic example of an element under predominantly physiological control, associated with the otolith organic matrix (Hüssy et al., 2020; Melancon et al., 2008; Reis-Santos et al., 2023). Experimental evidence confirms that waterborne Zn does not significantly increase otolith Zn concentrations, whereas dietary Zn does (Ranaldi and Gagnon, 2008). Its absence in *S. iracundus* is therefore unlikely to reflect environmental Zn deficiency. Rather, because Zn incorporation is primarily diet-derived and physiologically regulated, its absence may indicate that Zn was not deposited in the otolith due to the distinct metabolic demands and feeding regime of the migratory species.

Meanwhile, most elements' concentrations do not differ between *H. avius* and *A. latens* significantly. The greatest dissimilarity contribution belongs to Ti, which is relatively abundant in *A. latens* otoliths, but not in those of *S. iracundus* or *H. avius*. Ti is not known to be under strong physiological control and has been shown to reflect local environmental conditions (Geffen et al., 2003). The elements' marine geochemistry is dominated by particle reactivity and a benthic source. Dissolved Ti concentrations increase with depth due to diffusive fluxes from sediment pore waters, and resuspension of bottom sediments can locally enrich Ti in near-bottom waters (Orians et al., 1990; Skrabal, 2006). Given that *H. avius* and *A. latens* were collected at different depths and on different seamounts, the Ti/Ca difference between them is more likely to reflect local sediment and bottom-water conditions than a species-specific trait.

Thus, while the differences between *S. iracundus* and the sedentary species are driven by a complex multi-element signature (including both physiologically regulated and environment-derived elements), the finer-scale separation between *H. avius* and *A. latens* appears to be primarily environmental, reflecting their different catch localities.

Conclusions

The present study extends the available data on Sebastidae otolith chemistry, offering the first such records for three deep-sea species differing in their lifestyle. Differences in otolith element concentrations between the vertically migrating *S. iracundus* and the sedentary *A. latens* and *H. avius* were observed for most of the analyzed elements, forming a complex, multi-element signature rather than being driven by a single dominant marker. Several elements were completely absent in *S. iracundus* otoliths but present in the remaining species, or vice versa, reflecting a qualitative difference in elemental occurrence. Although the limited dataset prevents us from making any far-reaching conclusions, the distinct otolith composition of *S. iracundus* may be driven by its movement pattern, through both direct environmental influence and associated physiological processes. Further testing of this hypothesis requires larger sample sizes and analysis of elemental profiles measured along the fish growth axis (e.g., by laser ablation ICP-MS), which would allow the reconstruction of ontogenetic migrations and habitat shifts in these poorly studied deep-sea fishes.

Funding

This study received financial support from the Russian Science Foundation (grant No. 25-24-00262, https://rscf.ru/project/25-24-00262).

References

Afanasyev, P.K., Orlov, A.M. & Rolsky, A.Y. (2017) Otolith shape analysis as a tool for species identification and studying the population structure of different fish species. *Biology Bulletin*, 44 (7), 952–959. https://doi.org/10.1134/S1062359017080027

Aitchison, J. (1986) *The Statistical Analysis of Compositional Data*. Chapman and Hall, London.

Anderson, M.J. (2001) A new method for non-parametric multivariate analysis of variance. *Austral Ecology*, 26 (1), 32–46. https://doi.org/10.1111/j.1442-9993.2001.01070.pp.x

Barsukov, V.V. (1981) A brief review of the system of the subfamily of rockfishes (Sebastinae). *Journal of Ichthyology*, 21 (1), 1–26.

Barsukov, V.V. (2003) Annotated and illustrated check-list of rockfishes of the world. *Proceedings of the Zoological Institute of the Russian Academy of Sciences*, 295, 1–319.

Bath, G.E., Thorrold, S.R., Jones, C.M., Campana, S.E., McLaren, J.W. & Lam, J.W.H. (2000) Strontium and barium uptake in aragonitic otoliths of marine fish. *Geochimica et Cosmochimica Acta*, 64 (10), 1705–1714. https://doi.org/10.1016/S0016-7037(99)00419-6

Campana, S.E. (1999) Chemistry and composition of fish otoliths: pathways, mechanisms and applications. *Marine Ecology Progress Series*, 188, 263–297. https://doi.org/10.3354/meps188263

Campana, S.E. (2001) Accuracy, precision and quality control in age determination, including a review of the use and abuse of age validation methods. *Journal of Fish Biology*, 59 (2), 197–242. https://doi.org/10.1111/J.1095-8649.2001.TB00127.X

Campana, S.E., Chouinard, G.A., Hanson, J.M., Fréchet, A. & Brattey, J. (2000) Otolith elemental fingerprints as biological tracers of fish stocks. *Fisheries Research*, 46 (1–3), 343–357. https://doi.org/10.1016/S0165-7836(00)00158-2

Clarke, K.R. (1993) Non-parametric multivariate analyses of changes in community structure. *Australian Journal of Ecology*, 18 (1), 117–143. https://doi.org/10.1111/j.1442-9993.1993.tb00438.x

Dub, S.A. & Mizens, G.A. (2023) Geochemistry of rare earth elements and cerium anomaly in sedimentary marine carbonates: modern concepts. *Vestnik of Geosciences*, 11, 3–17. https://doi.org/10.19110/geov.2023.11.1

Dunn, O.J. (1964) Multiple comparisons using rank sums. *Technometrics*, 6 (3), 241–252. https://doi.org/10.1080/00401706.1964.10490181

Elderfield, H. & Pagett, R. (1986) Rare earth elements in ichthyoliths: Variations with redox conditions and depositional environment. *Science of the Total Environment*, 49, 175–197. https://doi.org/10.1016/0048-9697(86)90239-1

Farias, I., Perez-Mayol, S., Vieira, S., Morales-Nin, B., Tuset, V.M., García, A., González, J.A., Santana, J.I., Domínguez-Petit, R., Grau, A., et al. (2022) Ontogenetic spatial dynamics of the deep-sea teleost *Aphanopus carbo* in the NE Atlantic according to otolith geochemistry. *Deep Sea Research Part I: Oceanographic Research Papers*, 186, 103820. https://doi.org/10.1016/j.dsr.2022.103820

Friedrich, L.A. & Halden, N.M. (2008) Alkali element uptake in otoliths: A link between the environment and otolith microchemistry. *Environmental Science & Technology*, 42 (10), 3514–3518. https://doi.org/10.1021/es072093r

Froese, R. & Pauly, D., eds. (2026) *FishBase*. World Wide Web Electronic Publication. www.fishbase.org, version 06/2026).

Geffen, A.J., Jarvis, K., Thorpe, J.P., Leah, R.T. & Nash, R.D.M. (2003) Spatial differences in the trace element concentrations of Irish Sea plaice *Pleuronectes platessa* and whiting *Merlangius merlangus* otoliths. *Journal of Sea Research*, 50 (2–3), 245–254. https://doi.org/10.1016/j.seares.2003.06.001

Gillanders, B.M. (2005) Otolith chemistry to determine movements of diadromous and freshwater fish. *Aquatic Living Resources*, 18 (3), 291–300. https://doi.org/10.1051/alr:2005033

Hicks, T.L., Shamberger, K.E.F., Roark, E.B., Baco-Taylor, A. & Feely, R.A. (2025) Seawater carbonate chemistry along the Hawaiian-Emperor Seamount Chain in the North Pacific. *Journal of Geophysical Research: Oceans*, 130 (5), e2024JC021750. https://doi.org/10.1029/2024JC021750

Higgins, R.M., Isidro, E., Menezes, G.M. & Correia, A.T. (2013) Otolith elemental signatures indicate population separation in deep-sea rockfish, *Helicolenus dactylopterus* and *Pontinus kuhlii*, from the Azores. *Journal of Sea Research*, 83, 202–208. https://doi.org/10.1016/j.seares.2013.05.014

Høie, H., Otterlei, E. & Folkvord, A. (2004) Temperature-dependent fractionation of stable oxygen isotopes in otoliths of juvenile cod (*Gadus morhua* L.). *ICES Journal of Marine Science*, 61 (2), 243–251. https://doi.org/10.1016/j.icesjms.2003.11.006

Holm, S. (1979) A simple sequentially rejective multiple test procedure. *Scandinavian Journal of Statistics*, 6 (2), 65–70.

Hüssy K., Limburg K.E., de Pontual H., Thomas O.R.B., Cook P.K., Heimbrand Y., Blass M., Sturrock A.M. (2020). Trace element patterns in otoliths: the role of biomineralization. *Reviews in Fisheries Science & Aquaculture*, 29 (4): 445–477. https://doi.org/10.1080/23308249.2020.1760204

Ingram, T. (2011) Speciation along a depth gradient in a marine adaptive radiation. *Proceedings of the Royal Society B: Biological Sciences*, 278 (1705), 613–618. https://doi.org/10.1098/rspb.2010.1127

Kalish, J.M. (1989) Otolith microchemistry: validation of the effects of physiology, age and environment on otolith composition. *Journal of Experimental Marine Biology and Ecology*, 132 (3), 151–178. https://doi.org/10.1016/0022-0981(89)90126-3

Kastelle, C., Helser, T., TenBrink, T., Hutchinson, C., Goetz, B., Gburski, C. & Benson, I. (2020) Age validation of four rockfishes (genera *Sebastes* and *Sebastolobus*) with bomb-produced radiocarbon. *Marine & Freshwater Research*, 71 (10), 1355–1366. https://doi.org/10.1071/MF19280

Korostelev, N.B., Frey, P.H. & Orlov, A.M. (2020) Using different hard structures to estimate the age of deep-sea fishes: A case study of the Pacific flatnose, *Antimora microlepis* (Moridae, Gadiformes, Teleostei). *Fisheries Research*, 232, 105731. https://doi.org/10.1016/j.fishres.2020.105731

Korostelev, N.B. & Orlov, A.M. (2020) Micro- and ultramicroelemental content in otoliths of blue antimora *Antimora rostrata* and Pacific flatnose *A. microlepis* (Moridae, Teleostei). *Oceanology*, 60 (6), 798–802.

Korostelev, N.B., Volvenko, I.V., Maltsev, I.V. & Orlov, A.M. (2025) Brought to the surface from obscurity: the distribution and biology of *Coelorhinchus gilberti* (Macrouridae, Gadiformes, Teleostei) off the Emperor Seamounts (Northwestern Pacific). *Deep Sea Research Part II: Topical Studies in Oceanography*, 220, 105461. https://doi.org/10.1016/j.dsr2.2025.105461

Kruskal, W.H. & Wallis, W.A. (1952) Use of ranks in one-criterion variance analysis. *Journal of the American Statistical Association*, 47 (260), 583–621. https://doi.org/10.1080/01621459.1952.10483441

Kurbanov, Yu.K. (2025) Additions to the occurrence of two rare species of rockfish of the genus *Sebastes* (Sebastidae) in Pacific waters off the Kuril Islands. *Journal of Ichthyology*, 65 (3), 321–327. https://doi.org/10.1134/S0032945225700043

Kurbanov, Yu.K. & Mikhalyutin, E.A. (2022) New data on *Adelosebastes latens* (Sebastidae) from the region of the underwater elevations of the Hawaiian-Emperor Seamount Chain (Northern Pacific Ocean). *Journal of Ichthyology*, 62 (6), 1065–1074. https://doi.org/10.1134/S0032945221060084

Longmore, C., Fogarty, K., Neat, F., Brophy, D., Trueman, C.N., Milton, J.A. & Mariani, S. (2011) A comparison of otolith microchemistry and stable isotope approaches to population structure in a deep-sea fish, *Coryphaenoides rupestris*. *Marine Ecology Progress Series*, 442, 229–241. https://doi.org/10.1007/s10641-010-9674-1

Love, M.S., Yoklavich, M.M. & Thorsteinson, L.K. (2002) *The Rockfishes of the Northeast Pacific*. University of California Press, Berkeley.

Martin, G.B., Thorrold, S.R. & Jones, C.M. (2004) Temperature and salinity effects on strontium incorporation in otoliths of larval spot (*Leiostomus xanthurus*). *Canadian Journal of Fisheries and Aquatic Sciences*, 61 (1), 34–42. https://doi.org/10.1139/f03-143

McArdle, B.H. & Anderson, M.J. (2001) Fitting multivariate models to community data: a comment on distance-based redundancy analysis. *Ecology*, 82 (1), 290–297. https://doi.org/10.1890/0012-9658(2001)082[0290:FMMTCD]2.0.CO;2

Melancon S., Fryer B.J., Ludsin S.A., Gagnon J.E., Yang Z. (2008). Elemental signatures in otoliths of larval walleye (*Sander vitreus*) from Lake Erie: implications for natal origins and dispersal. *Canadian Journal of Fisheries and Aquatic Sciences*, 65 (12), 2726–2738. https://doi.org/10.1139/F08-162

Miller, J.A., Banks, M.A., Gomez-Uchida, D. & Shanks, A.L. (2005) A comparison of population structure in black rockfish (*Sebastes melanops*) as determined with otolith microchemistry and microsatellite DNA. *Canadian Journal of Fisheries and Aquatic Sciences*, 62 (10), 2189–2198. https://doi.org/10.1139/f05-133

NPFC (2024) *The Field Guide for Identifications of Fishes of the Emperor Seamount Chain Captured by Bottom Fisheries*. North Pacific Fisheries Commission, Tokyo.

Orians, K.J., Boyle, E.A. & Bruland, K.W. (1990) Dissolved titanium in the open ocean. *Nature*, 348, 322–325. https://doi.org/10.1038/348322a0

Orlov, A.M. & Tokranov, A.M. (2006) Spatial distribution and dynamics of catches of *Sebastes glaucus*, *S. iracundus* and *S. polyspinis* in Pacific waters off the Kuril Islands and Kamchatka. *Journal of Ichthyology*, 46 (8), 625–639. https://doi.org/10.1134/S0032945206080108

Orlov, A.M. & Tokranov, A.M. (2007) New data on distribution and biology of gray, angry, and northern rockfishes from the northwestern Pacific. In: *Biology, Assessment, and Management of North Pacific Rockfishes*. Alaska Sea Grant College Program, Fairbanks, pp. 59–85.

Orlov, A.M. & Tokranov, A.M. (2019) Checklist of deep-sea fishes of the Russian northwestern Pacific Ocean found at depths below 1000 m. *Progress in Oceanography*, 176, 102143. https://doi.org/10.1016/j.pocean.2019.102143

Orlov, A.M. & Tuponogov, V.N. (2026) Past and present ichthyological and fisheries research at the Emperor Seamounts: Lessons from the Soviet/Russian experience in the Central North Pacific. *Reviews in Fisheries Science & Aquaculture*, 34 (1), 94–111. https://doi.org/10.1080/23308249.2025.2523058

Orr, J.W. & Baker, A.J. (1996) New North American records of the northeast Pacific scorpaenids *Adelosebastes latens* and *Sebastes glaucus*. *Alaska Fisheries Research Bulletin*, 3 (2), 94–102.

Palarea-Albaladejo, J. & Martín-Fernández, J.A. (2015) zCompositions — R package for multivariate imputation of left-censored data under a compositional approach. *Chemometrics and Intelligent Laboratory Systems*, 143, 85–96. https://doi.org/10.1016/j.chemolab.2015.02.019

Pérez de Nanclares, M., Dessen, J.-E., Rørvik, K.-A., Thomassen, Y. & Thomassen, M.S. (2014) Feasibility of using rare earth elements (REEs) to mark and identify escaped farmed Atlantic salmon *Salmo salar* L. *Aquaculture Research*, 47 (6), 1–14. https://doi.org/10.1111/are.12647

R Core Team (2025) *R: A language and environment for statistical computing*. R Foundation for Statistical Computing, Vienna, Austria. Available from: https://www.R-project.org/ (accessed 10 August 2026).

Ranaldi, M.M. & Gagnon, M.M. (2008) Zinc incorporation in the otoliths of juvenile pink snapper (*Pagrus auratus* Forster): The influence of dietary versus waterborne sources. *Journal of Experimental Marine Biology and Ecology*, 360 (1), 56–62. https://doi.org/10.1016/j.jembe.2008.03.013

Reis-Santos, P., Gillanders, B.M., Sturrock, A.M., Izzo, C., Oxman, D.S., Lueders-Dumont, J.A., Hüssy, K., Tanner, S.E., Rogers, T., Doubleday, Z.A., Andrews, A.H., Trueman, C., Brophy, D., Thiem, J.D., Baumgartner, L.J., Willmes, M., Chung, M.T., Charapata, P., Johnson, R.C., Trumble, S., Heimbrand, Y., Limburg, K.E. & Walther, B.D. (2023) Reading the biomineralized book of life: Expanding otolith biogeochemical research and applications for fisheries and ecosystem-based management. *Reviews in Fish Biology and Fisheries*, 33 (2), 411–449. https://doi.org/10.1007/s11160-022-09720-z

Santificetur, C., Silva, R.M., Méndez, A., Pisonero, J. & Correia, A.T. (2026) Revealing ontogenetic vertical migration in deep-sea grenadiers (Macrouridae) from the southwestern Atlantic through otolith microchemistry. *Fishes*, 11 (5), 288. https://doi.org/10.3390/fishes11050288

Skrabal, S.A. (2006) Dissolved titanium distributions in the Mid-Atlantic Bight. *Marine Chemistry*, 102 (3–4), 218–229. https://doi.org/10.1016/j.marchem.2006.03.009

Secor, D.H. & Rooker, J.R. (2000) Is otolith strontium a useful scalar of life cycles in estuarine fishes? *Fisheries Research*, 46 (1–3), 359–371. https://doi.org/10.1016/S0165-7836(00)00159-4

Smith, J.N., Nelson, R. & Campana, S.E. (1991). The use of Pb-210/Ra-226 and Th-228/Ra-228 disequilibria in the ageing of otoliths of marine fish. In: Kershaw, P.J., Woodhead, D.S. (eds) Radionuclides in the study of marine processes. Springer, Dordrecht, pp. 350–359. https://doi.org/10.1007/978-94-011-3686-0_37

Snytko, V.A. (2001) *The Rockfishes of the Northern Part of Pacific Ocean*. TINRO-center, Vladivostok.

Stransky, C. (2004) *Stock separation and growth of redfish (genus Sebastes) in the North Atlantic by means of shape and elemental analysis of otoliths*. ICES CM/C:12. ICES Headquarters, Copenhagen, 14 pp.

Stransky, C., Garbe-Schönberg, C.-D. & Günther, D. (2005) Geographic variation and juvenile migration in Atlantic redfish inferred from otolith microchemistry. *Marine and Freshwater Research*, 56 (5), 677–691. https://doi.org/10.1071/MF04153

Swan, S.C., Geffen, A.J., Morales-Nin, B., Gordon, J.D.M., Shimmield, T., Sawyer, T. & Massutí, E. (2006) Otolith chemistry: an aid to stock separation of *Helicolenus dactylopterus* (bluemouth) and *Merluccius merluccius* (European hake) in the Northeast Atlantic and Mediterranean. *ICES Journal of Marine Science*, 63 (3), 504–513. https://doi.org/10.1016/j.icesjms.2005.08.012

Thorrold, S.R., Latkoczy, C., Swart, P.K. & Jones, C.M. (2001) Natal homing in a marine fish metapopulation. *Science*, 291 (5502), 297–299. https://doi.org/10.1126/science.291.5502.297

Tuset, V.M., Otero-Ferrer, J.L., Omez-Zurita, J.G., Venerus, L.A., Stransky, C., Imondi, R., Orlov, A.M., Ye, Z., Santschi, L., Afanasiev, P.K., Zhuang, L., Farre, M., Love, M.S. & Lombarte, A. (2016) Otolith shape lends support to the sensory drive hypothesis in rockfishes. *Journal of Evolutionary Biology*, 29 (10), 2083–2097. https://doi.org/10.1111/jeb.12932

Tzeng, W.N., Severin, K.P. & Wickström, H. (1997) Use of otolith microchemistry to investigate the environmental history of European eel *Anguilla anguilla*. *Marine Ecology Progress Series*, 149, 73–81. https://doi.org/10.3354/meps149073

Ward, J. H. (1963). Hierarchical Grouping to Optimize an Objective Function. *Journal of the American Statistical Association*, 58 (301), 236–244. https://doi.org/10.1080/01621459.1963.10500845

Widdrington, J.B., Reis-Santos, P., Morrongiello, J.R., Macdonald, J.I., Wakefield, C.B., Newman, S.J., Nicol, S.J. & Gillanders, B.M. (2025) Otolith growth chronologies reveal distinct environmental sensitivities between and within shallow- and deep-water snappers. *Reviews in Fish Biology and Fisheries*, 35 (1), 217–240. https://doi.org/10.1007/s11160-024-09898-4

Wu, L., Zhuang, W., Liu, Q., Zhang, J., Shen, X. & Li, S. (2024) Pilot study to reconstruct life history of *Diaphus thiollierei* from the Arabian Sea by otolith microstructure and microchemistry. *Acta Oceanologica Sinica*, 43 (12), 75–84. https://doi.org/10.1007/s13131-024-2307-x

Zhang, J., Amakawa, H. & Nozaki, Y. (1994) The comparative behaviors of yttrium and lanthanides in the seawater of the North Pacific. *Geophysical Research Letters*, 21 (24), 2677–2680. https://doi.org/10.1029/94GL02404

Supplement

Table S1. Concentrations of elements (ppm) in otoliths of *Sebastes iracundus*, *Helicolenus avius* and *Adelosebstes latens* (above the line, limits; below the line, mean ± standard deviation).

Element	*S. iracundus*	*H. avius*	*A. latens*
Ca	367500 – 385900 376725 ± 7544	366700 – 377200 371220 ± 4209	368700 – 381700 377540 ± 5289
Na	2980 – 3600 3145 ± 303	280 – 370 318 ± 43	370 – 460 420 ± 42
Sr	2800 – 3100 3003 ± 142	380 – 440 414 ± 24	370 – 430 398 ± 26
K	85.4 – 223.0 139.6 ± 58.8	16.0 – 22.0 18.6 ± 2.4	32.0 – 38.0 34.6 ± 2.2
P	393 – 630 538 ± 111	1000 – 1600 1240 ± 230	1200 – 1500 1340 ± 114
Si	29.0 – 92.0 49.6 ± 29.2	100 – 130 108 ± 13	68.0 – 92.0 81.0 ± 11.0
Mg	8.80 – 12.00 9.88 ± 1.45	18.0 – 36.0 26.0 ± 7.3	13.0 – 26.0 18.2 ± 5.1
Al	6.10 – 11.00 8.35 ± 2.02	26.0 – 37.0 29.6 ± 4.4	26.0 – 45.0 37.8 ± 7.9
Fe	7.60 – 120.0 38.7 ± 54.5	14.0 – 22.0 17.6 ± 3.6	21.0 – 30.0 25.6 ± 3.4
Ba	10.0 – 23.0 17.3 ± 5.4	4.80 – 7.50 5.96 ± 1.02	5.50 – 9.70 7.12 ± 1.56
Ti	0.400 – 0.580 0.473 ± 0.085	0.670 – 1.000 0.848 ± 0.123	2.40 – 5.30 3.40 ± 1.13
Ni	0.150 – 0.220 0.180 ± 0.029	0.400 – 0.850 0.548 ± 0.182	0.540 – 0.770 0.674 ± 0.086
Li	0.300 – 0.510 0.430 ± 0.091	0.730 – 1.500 1.082 ± 0.385	0.700 – 1.200 0.894 ± 0.192
Zn	—	3.50 – 5.60 4.52 ± 0.80	3.50 – 6.80 4.98 ± 1.47
Mn	0.030 – 0.050 0.036 ± 0.009	0.170 – 0.340 0.274 ± 0.069	0.300 – 0.420 0.376 ± 0.048
Cu	0.086 – 0.340 0.222 ± 0.109	0.240 – 0.570 0.322 ± 0.139	0.250 – 0.780 0.420 ± 0.216
Co	0.520 – 0.530 0.525 ± 0.006	0.520 – 0.600 0.552 ± 0.036	0.600 – 0.850 0.662 ± 0.106
B	0.280 – 0.660 0.415 ± 0.169	0.430 – 0.730 0.596 ± 0.129	0.520 – 0.780 0.640 ± 0.127
Ce	0.032†	0.080 – 0.720 0.264 ± 0.263	0.070 – 0.440 0.240 ± 0.137
La	—	0.200 – 0.430 0.274 ± 0.100	0.120 – 0.240 0.164 ± 0.057
Y	—	0.120 – 0.700 0.326 ± 0.229	0.150 – 0.580 0.342 ± 0.159
Ga	0.340 – 0.780 0.600 ± 0.192	—	—
Ge	0.110 – 0.140 0.125 ± 0.013	—	—
Rb	0.066 – 0.190 0.104 ± 0.058	—	—
Sc	0.045 – 0.400 0.216 ± 0.151	—	—

Table S2. Results of Kruskal–Wallis test for log-transformed element/Ca mass ratios in otoliths of three rockfish species (*Sebastes iracundus*, *Helicolenus avius*, *Adelosebastes latens*, from the Emperor Seamounts, northwestern Pacific. Significant differences after Benjamini–Hochberg correction ($p < 0.05$) are indicated in bold.

Element ratio	H	df	*p*-value	*p*-adjusted
Ti/Ca	11.571	2	0.0031	**0.0201**
K/Ca	11.571	2	0.0031	**0.0201**
Na/Ca	10.520	2	0.0052	**0.0201**
Si/Ca	10.260	2	0.0059	**0.0201**
Mn/Ca	10.063	2	0.0065	**0.0201**
Mg/Ca	9.651	2	0.0080	**0.0201**
Rb/Ca	9.651	2	0.0080	**0.0201**
Sc/Ca	9.651	2	0.0080	**0.0201**
Ga/Ca	9.651	2	0.0080	**0.0201**
Al/Ca	9.286	2	0.0096	**0.0201**
La/Ca	9.286	2	0.0096	**0.0201**
Co/Ca	9.071	2	0.0107	**0.0202**
Ni/Ca	8.966	2	0.0113	**0.0202**
Ba/Ca	8.691	2	0.0130	**0.0203**
Sr/Ca	8.691	2	0.0130	**0.0203**
P/Ca	8.280	2	0.0159	**0.0217**
Li/Ca	8.143	2	0.0171	**0.0217**
Y/Ca	8.143	2	0.0171	**0.0217**
Ce/Ca	8.051	2	0.0179	**0.0217**
Zn/Ca	8.006	2	0.0183	**0.0217**
Fe/Ca	4.843	2	0.0888	0.1009
B/Ca	4.200	2	0.1225	0.1331
Cu/Ca	1.971	2	0.3732	0.3887
Ge/Ca	1.871	2	0.3923	0.3923

Note: p-values were adjusted using Benjamini–Hochberg false discovery rate correction for multiple comparisons (24 tests). Bold font indicates statistical significance at $p = 0.05$ after correction.

Table S3. Pairwise comparisons (Dunn's test with Holm's correction) for log-transformed element/Ca ratios in otoliths of three rockfish species (*Sebastes iracundus*, *Helicolenus avius*, *Adelosebastes latens*) from the Emperor Seamount Chain, northwestern Pacific. Asterisks indicate significant differences (* $p < 0.05$; ** $p < 0.01$; *** $p < 0.001$).

Element ratio	Comparison	Z-statistic	*p*-adjusted
Ti/Ca	*A. latens* vs *S. iracundus*	3.385	0.002**
	H. avius vs *S. iracundus*	1.604	0.109
	A. latens vs *H. avius*	1.890	0.118
K/Ca	*A. latens* vs *S. iracundus*	-1.604	0.109
	H. avius vs *S. iracundus*	-3.385	0.002**
	A. latens vs *H. avius*	1.890	0.118
Na/Ca	*A. latens* vs *S. iracundus*	-1.746	0.161
	H. avius vs *S. iracundus*	-3.243	0.004**
	A. latens vs *H. avius*	1.587	0.112
Si/Ca	*A. latens* vs *S. iracundus*	1.122	0.262
	H. avius vs *S. iracundus*	3.118	0.006**
	A. latens vs *H. avius*	-2.117	0.069
Mn/Ca	*A. latens* vs *S. iracundus*	3.172	0.005**
	H. avius vs *S. iracundus*	1.817	0.138
	A. latens vs *H. avius*	1.436	0.151
Mg/Ca	*A. latens* vs *S. iracundus*	1.889	0.118
	H. avius vs *S. iracundus*	3.100	0.006**
	A. latens vs *H. avius*	-1.285	0.199
Rb/Ca	*A. latens* vs *S. iracundus*	-3.100	0.006**
	H. avius vs *S. iracundus*	-1.889	0.118
	A. latens vs *H. avius*	-1.285	0.199
Sc/Ca	*A. latens* vs *S. iracundus*	-3.100	0.006**
	H. avius vs *S. iracundus*	-1.889	0.118
	A. latens vs *H. avius*	-1.285	0.199
Ga/Ca	*A. latens* vs *S. iracundus*	-3.100	0.006**
	H. avius vs *S. iracundus*	-1.889	0.118
	A. latens vs *H. avius*	-1.285	0.199
Al/Ca	*A. latens* vs *S. iracundus*	3.029	0.007**
	H. avius vs *S. iracundus*	1.960	0.100
	A. latens vs *H. avius*	1.134	0.257
La/Ca	*A. latens* vs *S. iracundus*	1.960	0.100
	H. avius vs *S. iracundus*	3.029	0.007**
	A. latens vs *H. avius*	-1.134	0.257
Co/Ca	*A. latens* vs *S. iracundus*	2.976	0.009**
	H. avius vs *S. iracundus*	1.265	0.206
	A. latens vs *H. avius*	1.814	0.139
Ni/Ca	*A. latens* vs *S. iracundus*	2.958	0.009**
	H. avius vs *S. iracundus*	2.031	0.085
	A. latens vs *H. avius*	0.983	0.326
Ba/Ca	*A. latens* vs *S. iracundus*	-2.102	0.071
	H. avius vs *S. iracundus*	-2.886	0.012*
	A. latens vs *H. avius*	0.832	0.406
Sr/Ca	*A. latens* vs *S. iracundus*	-2.886	0.012*
	H. avius vs *S. iracundus*	-2.102	0.071
	A. latens vs *H. avius*	-0.832	0.406
P/Ca	*A. latens* vs *S. iracundus*	2.744	0.018*
	H. avius vs *S. iracundus*	2.245	0.049*
	A. latens vs *H. avius*	0.529	0.597
Li/Ca	*A. latens* vs *S. iracundus*	2.316	0.041*
	H. avius vs *S. iracundus*	2.673	0.023*
	A. latens vs *H. avius*	-0.378	0.706

..continued on the next page

Y/Ca	*A. latens* vs *S. iracundus*	2.673	0.023*
	H. avius vs *S. iracundus*	2.316	0.041*
	A. latens vs *H. avius*	0.378	0.706
Ce/Ca	*A. latens* vs *S. iracundus*	2.601	0.028*
	H. avius vs *S. iracundus*	2.388	0.034*
	A. latens vs *H. avius*	0.227	0.821
Zn/Ca	*A. latens* vs *S. iracundus*	2.530	0.034*
	H. avius vs *S. iracundus*	2.459	0.028*
	A. latens vs *H. avius*	0.076	0.940
Fe/Ca	*A. latens* vs *S. iracundus*	1.800	0.144
	H. avius vs *S. iracundus*	-0.053	0.957
	A. latens vs *H. avius*	1.965	0.148
B/Ca	*A. latens* vs *S. iracundus*	1.996	0.138
	H. avius vs *S. iracundus*	1.497	0.269
	A. latens vs *H. avius*	0.529	0.597
Cu/Ca	*A. latens* vs *S. iracundus*	1.390	0.494
	H. avius vs *S. iracundus*	0.606	0.545
	A. latens vs *H. avius*	0.832	0.811
Ge/Ca	*A. latens* vs *S. iracundus*	-0.517	0.605
	H. avius vs *S. iracundus*	0.766	0.887
	A. latens vs *H. avius*	-1.361	0.521

Note: p-values were adjusted using Holm's sequential Bonferroni correction. Holm's method controls the family-wise error rate across pairwise comparisons within each element.

Table S4. SIMPER results for pairwise comparisons of otolith elemental composition among three rockfish species. Values represent the average absolute difference in log10-transformed element/Ca ratios (Avg. difference), its standard deviation (SD), statistical significance based on 999 permutations (p-value), and the cumulative contribution to the total between-species dissimilarity (Cumulative contribution). Significant p-values (< 0.05) are shown in **bold**.

Species pair	Element/Ca	Avg. difference	SD	p-value	Cumulative contribution
S. iracundus – H. avius	Zn/Ca	0.00877	0.000392	**0.001**	0.095
	Y/Ca	0.00751	0.00152	**0.002**	0.176
	La/Ca	0.00744	0.000734	**0.001**	0.257
	Rb/Ca	0.00656	0.00106	**0.002**	0.328
	Sc/Ca	0.00624	0.00201	**0.002**	0.395
	Ce/Ca	0.00610	0.00219	**0.002**	0.461
	Na/Ca	0.00564	0.000364	**0.001**	0.522
	Ga/Ca	0.00534	0.000774	**0.002**	0.580
	Mn/Ca	0.00501	0.000789	**0.002**	0.634
	Sr/Ca	0.00486	0.000198	**0.002**	0.687
	K/Ca	0.00481	0.000911	**0.001**	0.739
	Al/Ca	0.00320	0.000599	**0.002**	0.774
	Ni/Ca	0.00271	0.000771	**0.002**	0.803
	Ba/Ca	0.00251	0.000847	**0.001**	0.830
	Mg/Ca	0.00237	0.000708	**0.001**	0.856
	Fe/Ca	0.00229	0.00160	0.060	0.881
	Li/Ca	0.00224	0.000933	**0.001**	0.905
	Si/Ca	0.00223	0.00114	**0.001**	0.929
	P/Ca	0.00211	0.000630	**0.003**	0.952
	Ti/Ca	0.00149	0.000537	0.997	0.968
	Cu/Ca	0.00141	0.00129	0.461	0.983
	B/Ca	0.00119	0.000728	**0.030**	0.996
	Ge/Ca	0.000199	0.000167	**0.016**	0.998
	Co/Ca	0.000167	0.000141	0.997	1.000
S. iracundus – A. latens	Zn/Ca	0.00886	0.000658	**0.001**	0.095
	Y/Ca	0.00778	0.00112	**0.001**	0.178
	Rb/Ca	0.00655	0.00105	**0.001**	0.249
	Sc/Ca	0.00623	0.00200	**0.001**	0.315
	Ce/Ca	0.00620	0.00181	**0.002**	0.382
	La/Ca	0.00610	0.000721	**0.002**	0.447
	Mn/Ca	0.00577	0.000575	**0.001**	0.509
	Ga/Ca	0.00534	0.000768	**0.001**	0.566
	Sr/Ca	0.00497	0.000207	**0.001**	0.619
	Na/Ca	0.00495	0.000318	**0.001**	0.672
	Ti/Ca	0.00477	0.000789	**0.001**	0.723
	Al/Ca	0.00371	0.000710	**0.001**	0.763
	K/Ca	0.00328	0.000871	**0.019**	0.798
	Ni/Ca	0.00324	0.000482	**0.001**	0.833
	Fe/Ca	0.00254	0.00121	**0.010**	0.860
	P/Ca	0.00227	0.000486	**0.001**	0.885
	Ba/Ca	0.00211	0.000880	**0.007**	0.907
	Cu/Ca	0.00180	0.00149	0.102	0.927
	Li/Ca	0.00180	0.000671	**0.030**	0.946
	Si/Ca	0.00160	0.000925	0.057	0.963
	Mg/Ca	0.00144	0.000668	0.255	0.978
	B/Ca	0.00129	0.000719	**0.018**	0.992
	Co/Ca	0.000541	0.000315	**0.003**	0.998
	Ge/Ca	0.000197	0.000132	**0.036**	1.000

..continued on the next page

H. avius – A. latens	Ti/Ca	0.00324	0.000751	**0.023**	0.163
	Ce/Ca	0.00198	0.00137	0.999	0.263
	Y/Ca	0.00152	0.00109	1.000	0.339
	K/Ca	0.00147	0.000287	0.982	0.414
	La/Ca	0.00135	0.000919	0.997	0.482
	Cu/Ca	0.00105	0.000898	0.859	0.534
	Mg/Ca	0.00103	0.000667	0.964	0.586
	Fe/Ca	0.000897	0.000514	0.989	0.632
	Mn/Ca	0.000825	0.000615	0.997	0.673
	Ni/Ca	0.000794	0.000425	0.997	0.713
	Li/Ca	0.000770	0.000596	0.997	0.752
	Si/Ca	0.000739	0.000378	0.967	0.789
	Al/Ca	0.000654	0.000401	0.997	0.822
	Na/Ca	0.000641	0.000370	0.997	0.855
	Zn/Ca	0.000627	0.000406	0.998	0.886
	Ba/Ca	0.000548	0.000418	0.998	0.914
	B/Ca	0.000528	0.000366	0.993	0.940
	P/Ca	0.000392	0.000248	0.999	0.960
	Co/Ca	0.000384	0.000336	0.117	0.980
	Sr/Ca	0.000211	0.000148	0.998	0.990
	Ge/Ca	4.86e-05	2.90e-05	0.986	0.993
	Ga/Ca	4.86e-05	2.90e-05	0.997	0.995
	Sc/Ca	4.85e-05	2.89e-05	0.997	0.998
	Rb/Ca	4.83e-05	2.88e-05	0.997	1.000

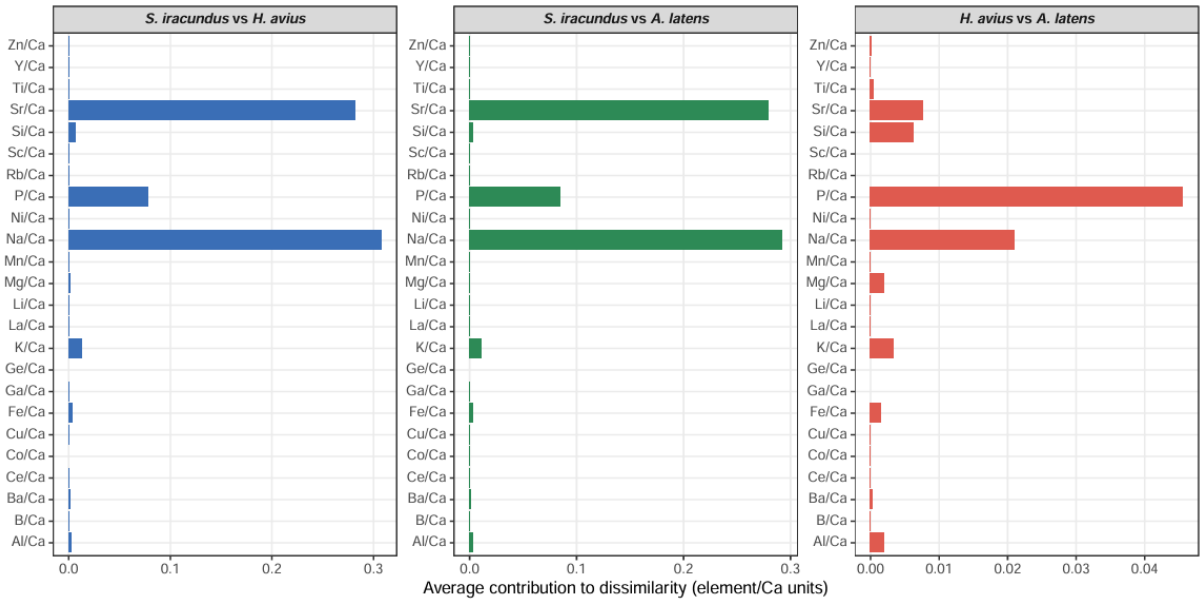


Figure S1. SIMPER analysis of otolith elemental composition among three rockfish species. Bars show the average contribution of each **untransformed** element/Ca ratio to the total between-species dissimilarity (Bray-Curtis index). Panels correspond to pairwise species comparisons; colors indicate the specific species pair; note that the scale is not consistent across panels.